Geophysical Research Letters

RESEARCH LETTER
10.1029/2024GL108444

Key Points:

- Smoke from intensive Canadian wildfires in early June of 2023 degraded the air quality of cities in eastern Canada and United States
- The wildfire smoke enhanced the development of the mid-latitude cyclone via smoke aerosol-radiation interaction
- The intensification and stagnation of the cyclone facilitated the transport of smoke to downwind cities in northeastern United States

Supporting Information:

Supporting Information may be found in the online version of this article.

Correspondence to:
X. Huang,
xinhuang@nju.edu.cn

Citation:
Wang, Z., Huang, X., Xue, L., Ding, K., Lou, S., Zhu, A., & Ding, A. (2024). Intensification of mid-latitude cyclone by aerosol-radiation interaction increases transport of Canadian wildfire smoke to northeastern US. *Geophysical Research Letters*, *51*, e2024GL108444. https://doi.org/10.1029/2024GL108444

Received 22 JAN 2024
Accepted 17 JUN 2024

Author Contributions:
Conceptualization: Zilin Wang, Xin Huang, Aijun Ding
Data curation: Lian Xue
Formal analysis: Sijia Lou
Investigation: Zilin Wang
Methodology: Zilin Wang, Lian Xue, Ke Ding, Anbao Zhu
Resources: Anbao Zhu
Software: Lian Xue, Sijia Lou
Supervision: Xin Huang, Aijun Ding
Visualization: Ke Ding
Writing – original draft: Zilin Wang
Writing – review & editing: Xin Huang, Aijun Ding

Intensification of Mid-Latitude Cyclone by Aerosol-Radiation Interaction Increases Transport of Canadian Wildfire Smoke to Northeastern US

Zilin Wang[1,2], Xin Huang[1,2,3], Lian Xue[1,2,3], Ke Ding[1,2], Sijia Lou[1,2,3], Anbao Zhu[1,2], and Aijun Ding[1,2,3]

[1]School of Atmospheric Sciences, Nanjing University, Nanjing, China, [2]Jiangsu Provincial Collaborative Innovation Center for Climate Change, Nanjing, China, [3]Frontiers Science Center for Critical Earth Material Cycling, Nanjing University, Nanjing, China

Abstract Wildfires have long been regarded as one chief culprit in regional air pollution, and pose great impacts on climate change. Although climate forcing of wildfire smoke has been widely investigated, its influence on synoptic systems remains unclear. Based on measurement and modeling analysis, the impact of wildfire smoke on the development of a mid-latitude cyclone was revealed for Canadian wildfires in early June of 2023. The radiative forcing induced by smoke at surface and in the atmosphere reached up to −150 and 100 W m^{-2}, posing opposite tendencies of atmospheric stratification over the land and ocean. Such perturbations contributed to the enhancement and stagnation of the cyclone, which favored the transport of smoke from the fire-intensive region, indicated by nearly 40% increment of $PM_{2.5}$ mass flux. With escalating wildfire risk in the future, the inclusion of smoke aerosols' impacts on meteorology in weather forecast models is of great importance.

Plain Language Summary Wildfires are uncontrolled fires that burn in the wildland vegetation, posing great challenges to regional air quality and global climate. Wildfire smoke has been known to exert great climate forcing via aerosol-radiation interaction yet its impact on synoptic scales needs further investigation. Here, based on comprehensive observations and modeling analysis for the extreme Canadian wildfires in early June of 2023, smoke aerosol is revealed to induce significant radiative forcing and yield opposite modifications of temperature stratification over the land and ocean, resulting in intensified and stagnant mid-latitude cyclone. Such perturbations favored the transport of smoke from fire-intensive region to downwind cities in Canada and United States, and the subsequent long-range transport dominated by the cyclone.

1. Introduction

Wildfires have been identified to increase across numerous regions of the globe in the past decade (Descals et al., 2022; Donovan et al., 2023; G. Liu et al., 2023; B. Zheng et al., 2023). Intensive wildfire activity with higher frequency and longer durations are strongly associated with climate change such as increasing air temperature, decreased precipitation and earlier spring snowmelt (Goss et al., 2020; Jolly et al., 2015; Westerling et al., 2006). As a kind of biomass burning (BB), wildfire can become dangerous and even deadly due to its rapid spread under favorable conditions, threatening human life and property security. Also, wildfire smoke contains many air pollutants such as carbon monoxide (CO) and particulate matter, which are of great concern for public health (Keywood et al., 2015; Reid et al., 2016). As has long been acknowledged, wildfires can "create their own weather" (Coen et al., 2013). Specifically, the heat and moisture released by the fire can feed back into the atmosphere, creating intense meteorological modifications such as strong wind and pyro-cumulonimbus (Cunningham & Reeder, 2009; Peterson et al., 2018). More importantly, large amount of smoke aerosols emitted from wildfire combustion can pose prominent climate forcing through their interactions with physical and chemical processes in the atmosphere (Carslaw et al., 2010).

Smoke aerosol generated from wildfires can perturb the atmospheric radiation budget and climate directly by reflecting and absorbing the solar radiation, often referred as aerosol-radiation interaction. Climate response to smoke aerosol had been evaluated previously. Wildfire aerosol emissions from the tropical region were reported to increase the global mean annual aerosol optical depth (AOD) by 10% and decrease net all-sky surface radiation by 1.3 W m^{-2}. Carbonaceous aerosols such as black carbon (BC) in smoke plume displayed strong radiative and climate effects by warming the middle and lower atmosphere (Y. Liu et al., 2014). A combination of tropospheric heating and surface cooling increased equatorial subsidence and weakened the Hadley circulation (Tosca et al., 2013). Wildfire aerosols can also force the climate indirectly by modifying cloud microphysics and reflectivity, namely aerosol-cloud interaction. Functioning as effective cloud condensation nuclei, wildfire aerosols have been shown to increase the concentration of cloud droplets, cloud lifetime, as well as decrease the cloud droplet size and thus delay the onset of the precipitation (Andreae et al., 2004; Kaufman & Fraser, 1997; Kaufman et al., 2005; Koren et al., 2004). Moreover, low cloud coverage, which plays a key role in the Earth-atmosphere energy balance, was found to be enhanced via its interaction with wildfire aerosols and monsoon in Southeast Asia (K. Ding et al., 2021).

While the impact of wildfire aerosols on climate has been well recognized, much less is known about its impact on meteorology at synoptic scales. Due to strong convection generated by fire activities, wildfire emissions could be lifted and injected above the planetary boundary layer into the free troposphere and transported across long distances by large-scale synoptic circulations (Hung et al., 2021; Shi et al., 2019; Sokolik et al., 2019). For example, the troposphere-wide cyclonic system is responsible for the long-range transport of Australian wildfire smoke and its entrance into stratosphere (Hirsch & Koren, 2021; Magaritz-Ronen & Raveh-Rubin, 2021). The dry intrusions behind mid-latitude cyclones can also result in downward transport of wildfire plume into the marine boundary layer (G. Zheng et al., 2020). While transported, wildfire aerosols tend to perturb the meteorology through its interaction with radiation and clouds. The inclusion of radiative effects of wildfire aerosols led to significant modifications of vertical profiles of temperature and moisture in cloud-free areas (G. Grell et al., 2011; Hodzic et al., 2007). Moreover, wildfire aerosols were reported to modify meteorology including air temperature, surface wind speed, air dryness, atmospheric stability and in turn promote the fire intensity as well as fire emissions, triggering positive fire-aerosol-weather feedback (A. Ding et al., 2013; Huang et al., 2020, 2023; Kochanski et al., 2019). Therefore, synoptic systems are not only responsible for the transport of smoke, but may also be affected by wildfire aerosols via radiative effect. However, the influence of the wildfire aerosols on mid-latitude synoptic systems such as extratropical cyclone and front remains unclear.

Under unusually warm and dry conditions, extreme fire seasons occurred over North America in summer of 2023. Accompanied by a strong mid-latitude cyclone, Quebec wildfires exerted a strong negative impact on air quality of eastern United States (US), and served as a good opportunity to investigate the influence of wildfire aerosols on the mid-latitude cyclone development and subsequent transport of smoke to downwind cities. In the following section, observational data sets and numerical modeling applied in this study are described. Next, the impact of smoke aerosol-radiation interaction on meteorology and the cyclone system is comprehensively analyzed, along with cyclone-dominated transport of wildfire smoke to downwind areas. Concluding remarks and discussions will be presented in Section 4.

2. Materials and Methods

2.1. Wildfire Inventory and Observational Data Sets

The information of Canadian wildfires is revealed by Fire Inventory from NCAR (FINN), which provides daily, 1 km resolution, global estimates of trace gas and particle emissions from open burning of biomass along with fire size and location based on satellite observations of active fires and land cover (Wiedinmyer et al., 2023). Fire detections from both MODIS and VIIRS satellite instruments are incorporated. Spatial and temporal variations of the wildfire smoke were illustrated by aerosol optical properties such as AOD provided by MODIS Aerosol Product MOD04_L2 and by ground-based automated radiometers from the Aerosol Robotic Network (AERONET). The Level 2 aerosol profile from the Cloud-Aerosol Lidar and Infrared Pathfinder Satellite Observation (CALIPSO version 4.51) were used to demonstrate vertical distribution and transport of wildfire aerosols. Daily average $PM_{2.5}$ concentration recorded by the Air Quality System of United States Environmental Protection Agency (US-EPA) was adopted to characterize the air pollution episode caused by wildfires. Integrated Surface Data Set composed of key meteorological parameters such as air temperature, relative humidity and wind archived at the National Climatic Data Center and atmospheric sounding observations collected by University of Wyoming were incorporated to perform weather analysis as well as model evaluation.

2.2. Numerical Experiments and Model Configuration

To shed more light on the impact of wildfire aerosols, numerical experiments are conducted using WRF-Chem version 3.7.1 in this study, which simulates trace gases and particulates interactively with the meteorological fields (G. A. Grell et al., 2005). The model has been widely applied to investigate the regional impacts of aerosols on meteorology (Huang et al., 2016; Z. Wang et al., 2019). Additional details of the model configuration including domain settings and selection of physical and chemical parameterization are elaborated in Text S1 of Supporting Information S1. Three parallel experiments EXP_FB, EXP_noFB and EXP_FB_noBB were performed to reveal the impact of wildfire aerosols on the mid-latitude cyclone system (Table S1 in Supporting Information S1). All experiments were conducted with identical domain setting and parameterizations summarized in Table S2 of Supporting Information S1. With wildfire emissions included, the EXP_FB considers aerosol-radiation interaction while EXP_noFB does not. In addition, wildfire emissions are excluded in EXP_FB_noBB to distinguish the influence of BB and anthropogenic emissions. The simulated meteorology and chemical fields were carefully evaluated and showed good agreements with ground-based and atmospheric sounding observations (Figures S3–S5 in Supporting Information S1). Moreover, optical properties of the wildfire aerosols including absorption and scattering parameters were evaluated with MODIS and CALIPSO observations as well (Figures S6–S8 in Supporting Information S1). Notably, sensitivity tests by doubling the fire emission intensity (Koplitz et al., 2018; Urbanski, 2014) showed better correspondence with multi-sourced observations (Figure S9 in Supporting Information S1) and was used for further analysis. With the intension to identify the transport pathways of wildfire smoke under the influence of wildfire aerosols, the Lagrangian particle dispersion model (LPDM) was operated using Hybrid Single-Particle Lagrangian Integrated Trajectory model (Stein et al., 2015). Meteorological fields from EXP_FB and EXP_noFB were adopted to drive LPDM to acquire 48-hr backward footprint of air masses arriving major cities in eastern United States including New York (40.7°N, 74.0°W), Albany (42.1°N, 73.8°W) and Trenton (40.2°N, 74.8°W).

3. Results

3.1. Air Pollution Caused by Record-Breaking Wildfires in Eastern North America

Canada suffers from record-breaking wildfires in summer of 2023 (CAMS, 2023). The fire season started early this year and burned over 156,000 km^2, which is 5 time more than its average, emitting 1.3 Pg CO_2 and 0.14 Pg CO_2 equivalent of other greenhouse gases (Z. Wang et al., 2023). The devastating wildfires were fueled by record high temperatures and widespread drought conditions across the country. Such extreme wildfires have been associated with climate change, namely warmer and drier weather contributing to the increase of flammability (Goss et al., 2020; Westerling et al., 2006). Among all the fires in eastern North America, wildfires burning in Quebec from 3 to 8 June has aroused the most attention since its smoke has filled skies with heavy haze for days over eastern United States, and caused an unprecedent air pollution episode in downwind cities such as New York (Figure S1 in Supporting Information S1, Figure 1c).

As shown in Figures 1a and 1b, more than 200 fires were ignited since 1 June in Quebec, and rapidly burnt out an area of 400 km^2 in the boreal forest. Due to the intensive combustion, massive trace gases such as CO and carbonaceous aerosols were released into the atmosphere. The average CO emissions during the burning period reached 8.4×10^4 Ton per day, which is far beyond its anthropogenic counterpart. Satellite derived AOD also exceed 2 at 550 nm, indicating high loadings of radiatively-active aerosols and thus a heavily polluted condition (Figure S1 in Supporting Information S1). After about 24-hr transport, the wildfire plume affected several states in the northeast of United States. Surface observed daily average $PM_{2.5}$ in major cities of US peaked on 7 June and exceeded 120 $\mu g\ m^{-3}$, which is 8 times higher than the guideline set by World Health Organization. A surge of ground-based AOD observations reached 2.5, larger than observations made during an intensive fire season in Europe (Hodzic et al., 2007). All suggested a severe air pollution episode related to the wildfire combustion.

It is worth noting that a persistent mid-latitude cyclone was responsible for the transport of the Quebec wildfire smoke to downwind cities (G. Zheng et al., 2020). During the pollution episode, a strong low-pressure center located to the northeast of United States (Figure S2 in Supporting Information S1). Such an extratropical cyclone with relatively cold air is a deep system stretching from the surface to 500 hPa. The northerly winds at the rear of the cyclone served as a bridge to bring plenty of wildfire smoke from fire-intensive region to downwind areas in eastern United States, worsening the air quality of the cities there. From 6 to 7 June, the low-pressure system deepened, as suggested by the lower sea level pressure as well as denser iso-geopotential lines at upper-level

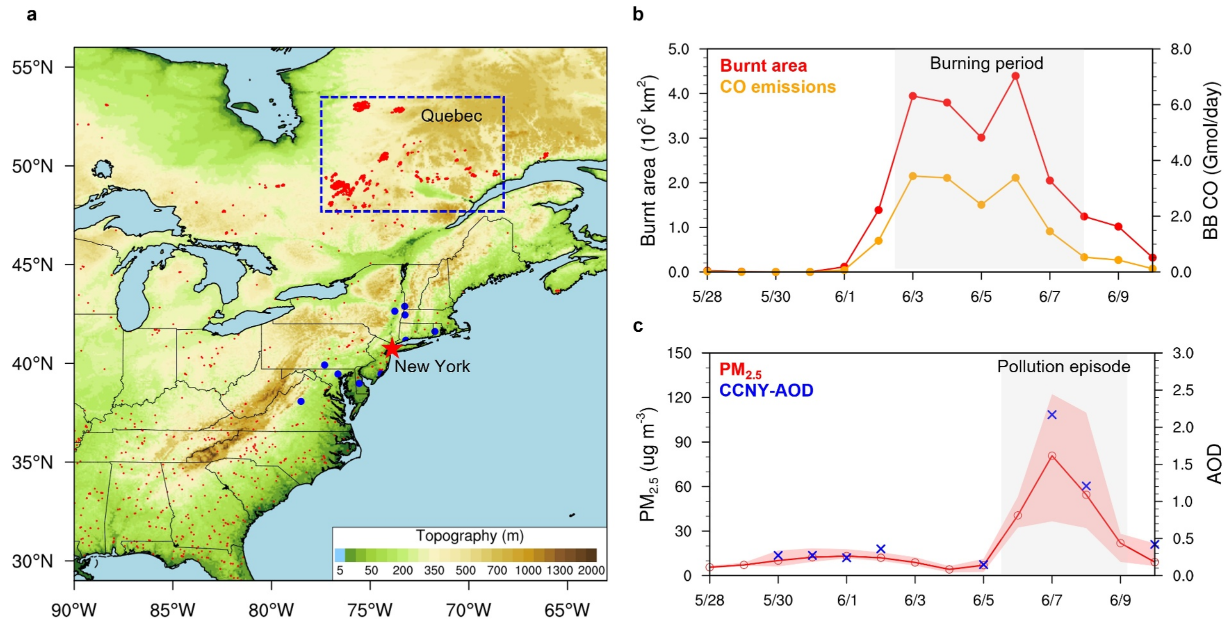

Figure 1. Canadian wildfires from 5 to 8 June 2023 and its impact on the air quality of downwind cities. (a) Detected fire spots during the burning period together with topography over eastern US and Canada. Blue dots and red star marked the location of air quality monitoring stations and the AERONET station at New York (CCNY), respectively. (b) Time series of burnt area and CO emissions from FINN within the fire-ravaged region, indicated by the blue rectangle in (a). (c) Time series of 24-hr average $PM_{2.5}$ concentration and aerosol optical depth at 440 nm measured at downwind AERONET stations.

atmosphere. Moreover, instead of moving eastward along with westerly jet, the low-pressure system remained stagnant. Both conditions were unfavorable for the dispersion and elimination of the smoke plume. Therefore, the cities were shrouded with heavy and long-lasting wildfire smoke (Figure 1c). Given the significant radiative effect of smoke aerosol, its impact on the mid-latitude cyclone needs further investigation.

3.2. The Impact of Smoke Aerosol-Radiation Interaction on the Cyclone System

To reveal the influence of the wildfire aerosols on the development of the mid-latitude cyclone system, numerical simulations were conducted using WRF-Chem. Thorough evaluation of modeling results demonstrated that the model could generally reproduce the evolvement of synoptic processes as well as wildfire smoke during this episode except for EXP_FB_noBB (Figures S3–S8 in Supporting Information S1). The surface $PM_{2.5}$ concentration were largely underestimated in EXP_FB_noBB with no peak values, indicating the major contribution of wildfire emissions to the air quality degradation. The simulated column $PM_{2.5}$ concentration resembled satellite derived AOD and was greatly shaped by the mid-latitude cyclone, which transported the smoke from fire-intensive region to eastern US as well as the Atlantic Ocean (Figure 2a).

Aerosols from wildfires consist of a wide variety of absorptive and scattering particles, mostly in the form of organic and BC. These aerosols are found to greatly perturb the radiation transfer (Figure 2b). To be specific, the radiative forcing was about -150 W m^{-2} at the ground surface and 100 W m^{-2} in the atmosphere, with a net energy loss at the top of the atmosphere. Such radiative forcings were also identified during other wildfire events based on observations or simulations (Gorchakov et al., 2014; Péré et al., 2014). However, air temperature showed different responses over the land and ocean. The smoke shading effect led to daytime surface cooling by 1°C while the absorbing aerosols such as BC tended to heat the upper atmosphere and caused atmospheric warming by about 0.5°C at 700 hPa (Figures 2c and 2d). Such modifications of the atmospheric stratification were also reported by a numerical study conducted by Kochanski et al. (2019) using a coupled fire-atmosphere model, and were also reflected by the atmospheric sounding profile well captured in EXP_FB experiment only (Figure S3 in Supporting Information S1). As for the ocean, near-surface cooling was negligible while the atmospheric warming prevailed. Such disparities could be attributed to the different thermodynamic properties of the land and ocean (Q. Ding et al., 2019; Z. Wang et al., 2020). Due to greater heat capacity, the ocean is less sensitive to the reduction of incident solar radiation reaching its surface, further

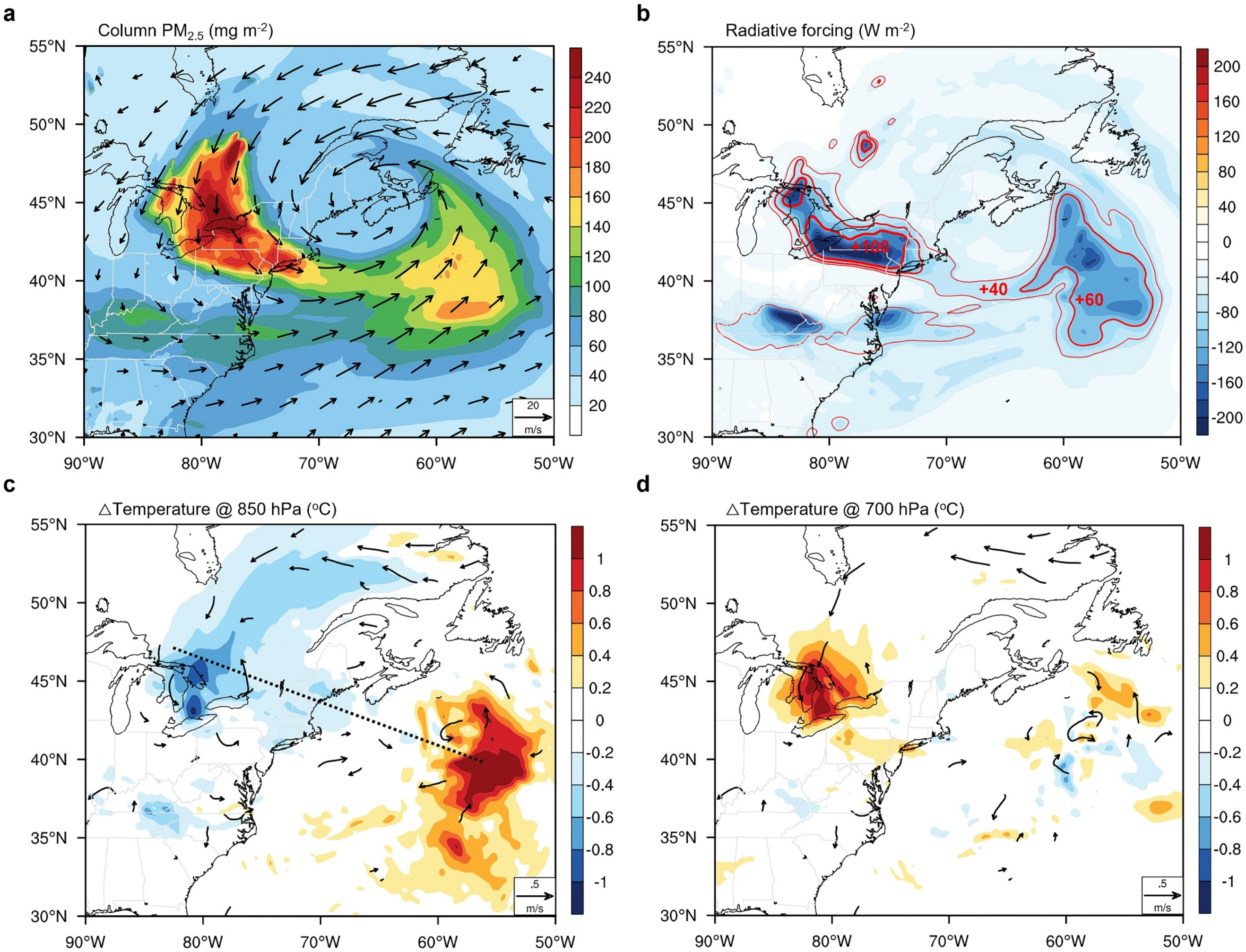

Figure 2. Meteorological perturbations induced by smoke aerosol-radiation interaction during 12:00–16:00 LT on 7 June. (a) Simulated $PM_{2.5}$ column concentration and wind field at 850 hPa. (b) Radiative forcing of smoke aerosols at the surface (shading) and in the atmosphere (contour line). Air temperature and wind field perturbations caused by smoke aerosols at 850 and 700 hPa are shown in (c) and (d). Red line in (c) marks the cross-section shown in Figure 3b.

verified by little response of surface sensible and latent heat flux over the ocean in contrast to land, which served as the predominant heating source of near-surface atmosphere (Figure S10 in Supporting Information S1). Therefore, the surface cooling is absent while atmospheric warming caused by absorbing aerosols dominated the modifications in stability over the ocean.

Such changes of the atmospheric stratification forced a counter-clockwise circulation of wind anomaly, suggesting an enhancement of the mid-latitude cyclone (Figures 2c and 2d). The upper-level warming and lower-level cooling over the land contributed to a more stable stratification and downward motions of the air masses at the rear of the cyclone (J. Wang et al., 2023; Z. Wang et al., 2018), indicated by a varation of -4×10^{-3} m s^{-1} in vertical velocity. On the contrary, the entire warming over the ocean resulted in an unstable atmosphere with upward air motions at the front of the cyclone with 6×10^{-3} m s^{-1} velocity anomaly in vertical direction. Therefore, the upper-level trough was intensified by the convergence (divergence) at the front (rear) of itself, which regulated the development of the cyclone. Similar effect has also been reported during a super dust storm in eastern Asia (Chen et al., 2023). The larger temperature gradient at 850 hPa caused by smoke aerosols may also contribute to the deepening via cold advection. The intensification was further confirmed by the reduction of sea level pressure and the geopotential height (Figures 3a and 3b). At 500 hPa, the geopotential height at the center of the cyclone in EXP_FB appears lower than that in EXP_noFB, with the average geopotential height being 5,412 and 5,421 gpm, respectively (Figure 3c). The relative vorticity, which represent the spin and rotation of the air

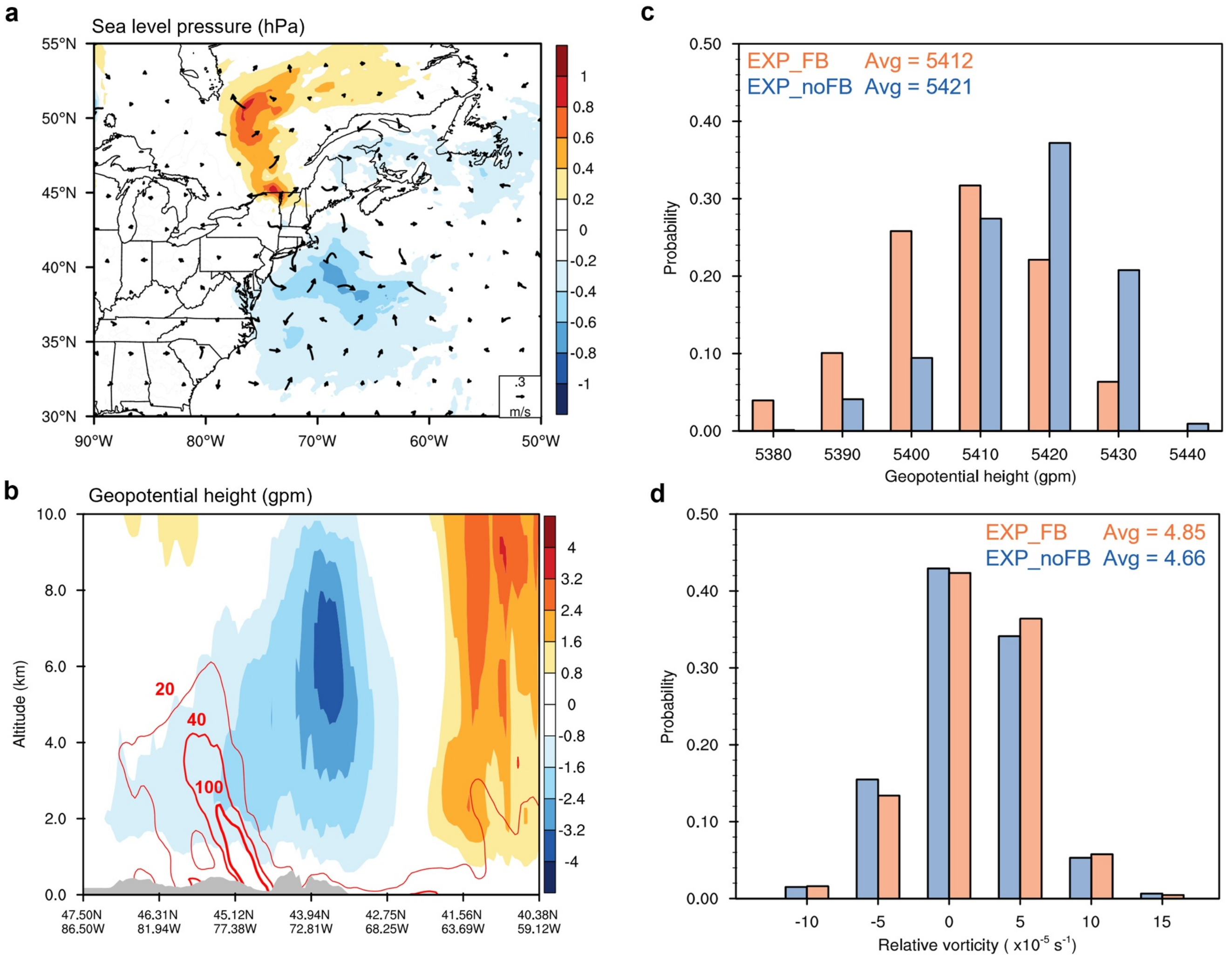

Figure 3. The impact of smoke aerosol-radiation interaction on the mid-latitude cyclone during 12:00–16:00 LT on 7 June. (a) Perturbations in sea level pressure and surface wind. (b) Changes in geopotential height along the cross-section through the cyclone system. The location of the cross-section is marked in Figure 2c with black dashed line. Vertical distribution of smoke aerosols (units: μg m^{-3}) are displayed in red contour lines. Probability distribution histogram of geopotential height at the center of the cyclone (c) and relative vorticity of the cyclone (d) at 500 hPa in different scenarios.

masses, are also derived from the wind fields. As shown in Figure 3d, the smoke aerosol-radiation interaction tends to increase the relative vorticity, suggesting the enhancement of the cyclone system as well.

3.3. Enhanced Transport of Wildfire Smoke to Downwind Cities

The smoke-aerosol radiation interaction affect not only the intensity but also the stagnation of the mid-latitude cyclone. Here, the location of the cyclone was estimated as the position of the lowest pressure at 500 hPa and marked on the map with its corresponding time (Figure 4a). Compared to the moving trail of the cyclone center in EXP_noFB, the location of cyclone falls to the west in EXP_FB, especially from 12:00 LT on 7 June to the morning of 8 June when the wildfire smoke was the most widespread. The translation speed of the mid-latitude cyclone is 7.9 km hr^{-1}, slower than 9.2 km hr^{-1} which is not affected by smoke aerosol-radiation interaction, making it more favorable for the transport of wildfire smoke from fire-intensive region. The 48-hr backward footprint calculated using LPDM driven by meteorological fields from EXP_FB and EXP_noFB provided more evidence (Figure 4b). The air masses arriving at New York were more likely to originate from the fire-intensive region when considering the impact of smoke aerosol-radiation interaction on the cyclone development on 7 June. Other cities in eastern US such as Albany and Trenton have analogous results which are not shown here.

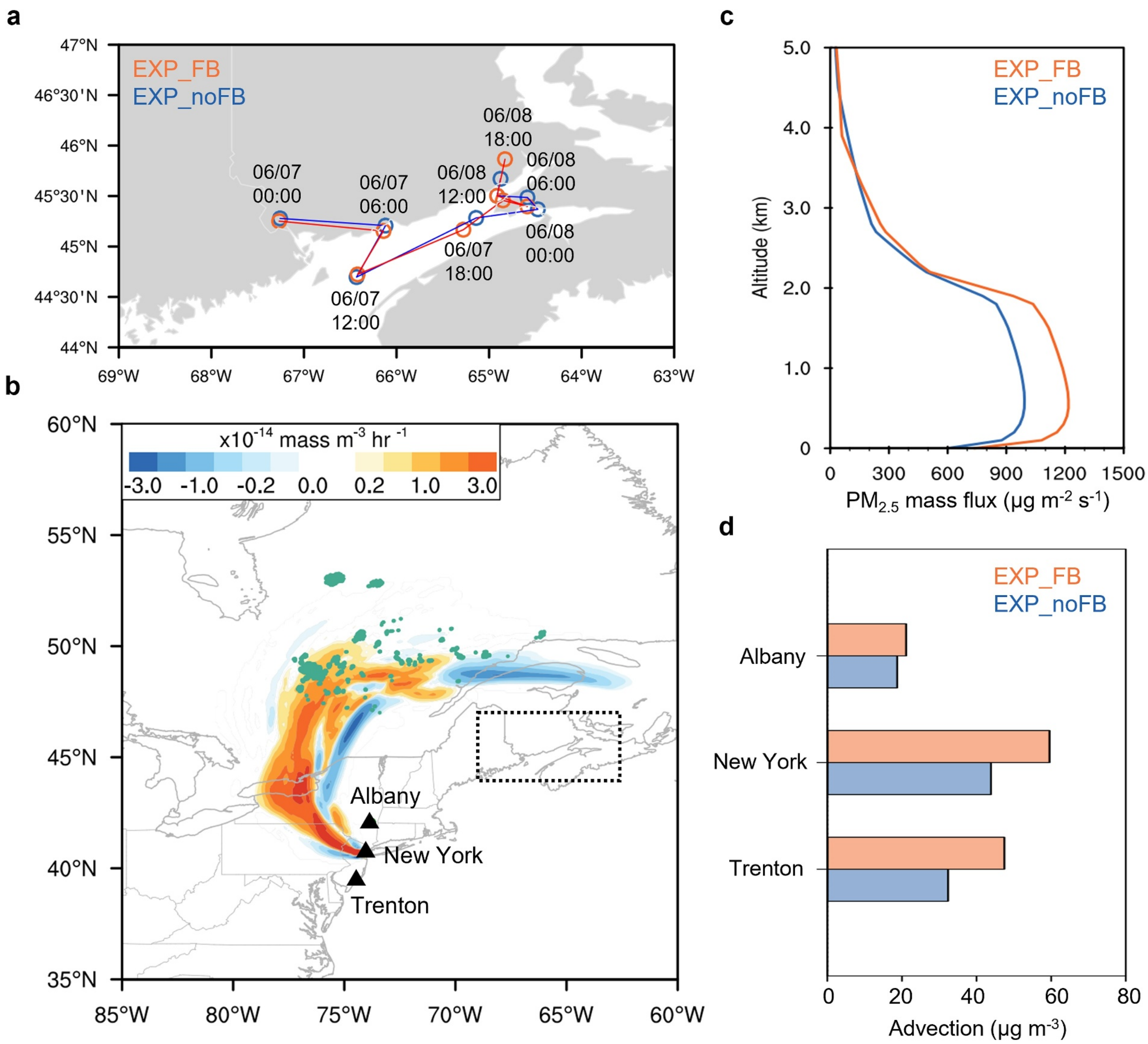

Figure 4. The stagnation of the mid-latitude cyclone greatly affected the transport of wildfire smoke during 10:00–24:00 LT on 7 June. (a) Estimated location of the cyclone center during the pollution episode. The scope and location of this domain is indicated by the rectangle in (b). (b) The difference of 48-hr backward footprint between EXP_FB and EXP_noFB initiated from New York. Green dots represent detected fire spots during the burning period. (c) Vertical profile of the $PM_{2.5}$ mass flux in New York in EXP_FB and EXP_noFB simulations. (d) Diagnosed contribution of advection process to the total surface $PM_{2.5}$ concentration on 7 June in three cities in different simulations.

Therefore, the intensified mid-latitude cyclone tends to be more stagnant under the influence of smoke aerosol-radiation interaction and thus exacerbated the air pollution in downwind cities of eastern United States.

Compared with the synoptic background environment of a mid-latitude cyclone system, smoke aerosol may not be a strong external forcing. However, due to smoke aerosol-radiation interaction, modifications of the intensity and stagnation of the cyclone do make a difference on the transport of the wildfire smoke to the downwind areas. To reveal its influence on the transport, mass flux of smoke aerosol, represented by $PM_{2.5}$ concentration multiplied by wind speed, was investigated. The vertical profile of the mass flux showed great differences below 2 km (Figure 4c). Specifically, the aerosol mass flux increased by 38% within the boundary layer. As shown in Figure 4d, the diagnostic analysis of the $PM_{2.5}$ at three cities all emphasized the importance of advection processes, which is also enhanced by 26% under the influence of smoke aerosol-radiation interaction.

4. Conclusions and Discussions

North America suffers from intensive wildfires in the summer of 2023, exerting great impacts on regional air quality. Although climate forcing of wildfire smoke has been widely acknowledged, its impact on synoptic systems remains unclear. In early June of 2023, Canadian wildfires accompanied by a mid-latitude cyclone system significantly degraded the air quality in downwind cities of Canada and United States. Based on comprehensive analysis of multiple observational data sets and meteorology-chemistry coupled numerical simulations, the impact of smoke aerosol-radiation interaction on the cyclone development was investigated in-depth. The direct radiative effect of smoke aerosols in all posed radiative forcing of −150 and 100 W m^{-2} at ground surface and in the atmosphere, respectively, yet exerted opposite tendencies of atmospheric stratification over the land and ocean. Such perturbations contributed to the enhancement of upper-level trough and hence the cyclone, indicated by the increase of geopotential height and the relative vorticity around the center of the cyclone. Moreover, the location of the cyclone was also affected, facilitating the transport of wildfire smoke from the fire -intensive region to downwind cities, suggested by nearly 40% increment of $PM_{2.5}$ mass flux.

Moreover, the intensification of mid-latitude cyclone can also amplify the long-range transport of aerosols via frontal systems especially warm conveyor belts, which could lift air pollutants from boundary layer into the free troposphere (A. Ding et al., 2009). Since the cyclone system was often accompanied by abundant clouds, to qualitatively understand the relative contribution of aerosol-radiation interaction and aerosol-cloud interaction, multiple sensitivity experiments have been conducted. Compared with aerosol-radiation interaction discussed above, the impact of smoke aerosols on cloud microphysics such as cloud droplet number concentration and cloud water mixing ratio are limited, probably due to little overlay of the smoke and clouds under such synoptic conditions (Figure S12 in Supporting Information S1). The absorption of smoke aerosol was overestimated by about 25% due to internal mixing assumption made in the model while the aerosol vertical distribution applied may vary 10%–30% resulted from the weakened satellite retrieved signal at lower atmosphere (Young et al., 2013; Zeng et al., 2024). More efforts are still in need for observation and model development for wildfire aerosols at finer spatiotemporal resolution. Considering the escalating risk of wildfires in many regions of the globe under the changing climate, it is of great importance to take synoptic-scale radiative effect of smoke aerosol into account. Furthermore, the inclusion of such aerosols' effect in both weather and air quality forecasting models may help improve the predictability of weather and environmental extreme events.

Data Availability Statement

The daily global fire emissions used in this study are derived from FINN v2.5 (Wiedinmyer & Emmons, 2022). The global hourly surface meteorological data are available at National Centers for Environmental Information (2023) and the radiosonde observations are archived at Department of Atmospheric Science, University of Wyoming (Department of Atmospheric Science, 2015). The AOD measurements come from AERONET stations (Giles et al., 2019) and the MODIS with a spatial resolution of 10 km (Levy & Hsu, 2015). The Level 2 cloud and aerosol profile from CALIPSO can be ordered at Atmospheric Science Data Center (NASA/LARC/SD/ASDC, 2018). The daily surface $PM_{2.5}$ concentration was observed and provided by US-EPA (U.S. Environmental Protection Agency, 2023). Model simulation data used in this study are available upon request.

Acknowledgments

This work was supported by the National Natural Science Foundation of China (42325506 and 42305117) and Fundamental Research Funds for the Central Universities (14380198). We are grateful to the high-performance computing center of collaborative innovation center of advanced microstructures of Nanjing University for conducting analysis and calculations in this paper. We would also like to thank US EPA project for collecting air quality data, Aerosol Robotic Network program for providing ground-based aerosol products, and MODIS/CALIPSO science team for production and distribution of satellite observations.

References

Andreae, M. O., Rosenfeld, D., Artaxo, P., Costa, A. A., Frank, G. P., Longo, K. M., & Silva-Dias, M. A. (2004). Smoking rain clouds over the Amazon. *Science*, *303*(5662), 1337–1342. https://doi.org/10.1126/science.1092779

CAMS. (2023). *A record-breaking boreal wildfire season*. Copernicus Atmosphere Monitoring Service. Retrieved from https://atmosphere.copernicus.eu/record-breaking-boreal-wildfire-season

Carslaw, K. S., Boucher, O., Spracklen, D. V., Mann, G. W., Rae, J. G. L., Woodward, S., & Kulmala, M. (2010). A review of natural aerosol interactions and feedbacks within the Earth system. *Atmospheric Chemistry and Physics*, *10*(4), 1701–1737. https://doi.org/10.5194/acp-10-1701-2010

Chen, Y., Chen, S., Zhou, J., Zhao, D., Bi, H., Zhang, Y., et al. (2023). A super dust storm enhanced by radiative feedback. *npj Climate and Atmospheric Science*, *6*(1), 90. https://doi.org/10.1038/s41612-023-00418-y

Coen, J. L., Cameron, M., Michalakes, J., Patton, E. G., Riggan, P. J., & Yedinak, K. M. (2013). WRF-fire: Coupled weather–wildland fire modeling with the weather research and forecasting model. *Journal of Applied Meteorology and Climatology*, *52*(1), 16–38. https://doi.org/10.1175/JAMC-D-12-023.1

Cunningham, P., & Reeder, M. J. (2009). Severe convective storms initiated by intense wildfires: Numerical simulations of pyro-convection and pyro-tornadogenesis. *Geophysical Research Letters*, *36*(12), L12812. https://doi.org/10.1029/2009gl039262

Department of Atmospheric Science. (2015). University of Wyoming upper-air observations database [Dataset]. *University of Wyoming*. Retrieved from http://weather.uwyo.edu/upperair

Descals, A., Gaveau, D. L. A., Verger, A., Sheil, D., Naito, D., & Peñuelas, J. (2022). Unprecedented fire activity above the Arctic Circle linked to rising temperatures. *Science*, *378*(6619), 532–537. https://doi.org/10.1126/science.abn9768

Ding, A., Fu, C., Yang, X., Sun, J., Petäjä, T., Kerminen, V. M., et al. (2013). Intense atmospheric pollution modifies weather: A case of mixed biomass burning with fossil fuel combustion pollution in eastern China. *Atmospheric Chemistry and Physics*, *13*(20), 10545–10554. https://doi.org/10.5194/acp-13-10545-2013

Ding, A., Wang, T., Xue, L., Gao, J., Stohl, A., Lei, H., & Zhang, X. (2009). Transport of north China air pollution by midlatitude cyclones: Case study of aircraft measurements in summer 2007. *Journal of Geophysical Research*, *114*(D8), D08304. https://doi.org/10.1029/2009JD012339

Ding, K., Huang, X., Ding, A., Wang, M., Su, H., Kerminen, V. M., et al. (2021). Aerosol-boundary-layer-monsoon interactions amplify semi-direct effect of biomass smoke on low cloud formation in Southeast Asia. *Nature Communications*, *12*(1), 6416. https://doi.org/10.1038/s41467-021-26728-4

Ding, Q., Sun, J., Huang, X., Ding, A., Zou, J., Yang, X., & Fu, C. (2019). Impacts of black carbon on the formation of advection–radiation fog during a haze pollution episode in eastern China. *Atmospheric Chemistry and Physics*, *19*(11), 7759–7774. https://doi.org/10.5194/acp-19-7759-2019

Donovan, V. M., Crandall, R., Fill, J., & Wonkka, C. L. (2023). Increasing large wildfire in the eastern United States. *Geophysical Research Letters*, *50*(24). https://doi.org/10.1029/2023gl107051

Giles, D. M., Sinyuk, A., Sorokin, M. G., Schafer, J. S., Smirnov, A., Slutsker, I., et al. (2019). Advancements in the Aerosol Robotic Network (AERONET) Version 3 database – Automated near-real-time quality control algorithm with improved cloud screening for Sun photometer aerosol optical depth (AOD) measurements [Dataset]. *Atmospheric Measurement Techniques*, *12*(1), 169–209. https://doi.org/10.5194/amt-12-169-2019

Gorchakov, G. I., Sitnov, S. A., Sviridenkov, M. A., Semoutnikova, E. G., Emilenko, A. S., Isakov, A. A., et al. (2014). Satellite and ground-based monitoring of smoke in the atmosphere during the summer wildfires in European Russia in 2010 and Siberia in 2012. *International Journal of Remote Sensing*, *35*(15), 5698–5721. https://doi.org/10.1080/01431161.2014.945008

Goss, M., Swain, D. L., Abatzoglou, J. T., Sarhadi, A., Kolden, C. A., Williams, A. P., & Diffenbaugh, N. S. (2020). Climate change is increasing the likelihood of extreme autumn wildfire conditions across California. *Environmental Research Letters*, *15*(9), 094016. https://doi.org/10.1088/1748-9326/ab83a7

Grell, G., Freitas, S. R., Stuefer, M., & Fast, J. (2011). Inclusion of biomass burning in WRF-Chem: Impact of wildfires on weather forecasts. *Atmospheric Chemistry and Physics*, *11*(11), 5289–5303. https://doi.org/10.5194/acp-11-5289-2011

Grell, G. A., Peckham, S. E., Schmitz, R., McKeen, S. A., Frost, G., Skamarock, W. C., & Eder, B. (2005). Fully coupled "online" chemistry within the WRF model. *Atmospheric Environment*, *39*(37), 6957–6975. https://doi.org/10.1016/j.atmosenv.2005.04.027

Hirsch, E., & Koren, I. (2021). Record-breaking aerosol levels explained by smoke injection into the stratosphere. *Science*, *371*(6535), 1269–1274. https://doi.org/10.1126/science.abe1415

Hodzic, A., Madronich, S., Bohn, B., Massie, S., Menut, L., & Wiedinmyer, C. (2007). Wildfire particulate matter in Europe during summer 2003: Meso-scale modeling of smoke emissions, transport and radiative effects. *Atmospheric Chemistry and Physics*, *7*(15), 4043–4064. https://doi.org/10.5194/acp-7-4043-2007

Huang, X., Ding, A., Liu, L., Liu, Q., Ding, K., Niu, X., et al. (2016). Effects of aerosol–radiation interaction on precipitation during biomass-burning season in East China. *Atmospheric Chemistry and Physics*, *16*(15), 10063–10082. https://doi.org/10.5194/acp-16-10063-2016

Huang, X., Ding, A., Wang, Z., Ding, K., Gao, J., Chai, F., & Fu, C. (2020). Amplified transboundary transport of haze by aerosol–boundary layer interaction in China. *Nature Geoscience*, *13*(6), 428–434. https://doi.org/10.1038/s41561-020-0583-4

Huang, X., Ding, K., Liu, J., Wang, Z., Tang, R., Xue, L., et al. (2023). Smoke-weather interaction affects extreme wildfires in diverse coastal regions. *Science*, *379*(6631), 457–461. https://doi.org/10.1126/science.add9843

Hung, W.-T., Lu, C.-H., Alessandrini, S., Kumar, R., & Lin, C.-A. (2021). The impacts of transported wildfire smoke aerosols on surface air quality in New York State: A multi-year study using machine learning. *Atmospheric Environment*, *259*, 118513. https://doi.org/10.1016/j.atmosenv.2021.118513

Jolly, W. M., Cochrane, M. A., Freeborn, P. H., Holden, Z. A., Brown, T. J., Williamson, G. J., & Bowman, D. M. J. S. (2015). Climate-induced variations in global wildfire danger from 1979 to 2013. *Nature Communications*, *6*(1), 7537. https://doi.org/10.1038/ncomms8537

Kaufman, Y. J., & Fraser, R. S. (1997). The effect of smoke particles on clouds and climate forcing. *Science*, *277*(5332), 1636–1639. https://doi.org/10.1126/science.277.5332.1636

Kaufman, Y. J., Koren, I., Remer, L. A., Rosenfeld, D., & Rudich, Y. (2005). The effect of smoke, dust, and pollution aerosol on shallow cloud development over the Atlantic Ocean. *Proceedings of the National Academy of Sciences of the USA*, *102*(32), 11207–11212. https://doi.org/10.1073/pnas.0505191102

Keywood, M., Cope, M., Meyer, C. P. M., Iinuma, Y., & Emmerson, K. (2015). When smoke comes to town: The impact of biomass burning smoke on air quality. *Atmospheric Environment*, *121*, 13–21. https://doi.org/10.1016/j.atmosenv.2015.03.050

Kochanski, A. K., Mallia, D. V., Fearon, M. G., Mandel, J., Souri, A. H., & Brown, T. (2019). Modeling wildfire smoke feedback mechanisms using a coupled fire-atmosphere model with a radiatively active aerosol scheme. *Journal of Geophysical Research: Atmospheres*, *124*(16), 9099–9116. https://doi.org/10.1029/2019jd030558

Koplitz, S. N., Nolte, C. G., Pouliot, G. A., Vukovich, J. M., & Beidler, J. (2018). Influence of uncertainties in burned area estimates on modeled wildland fire $PM_{2.5}$ and ozone pollution in the contiguous U.S. *Atmospheric Environment*, *191*, 328–339. https://doi.org/10.1016/j.atmosenv.2018.08.020

Koren, I., Kaufman, Y. J., Remer, L. A., & Martins, J. V. (2004). Measurement of the effect of Amazon smoke on inhibition of cloud formation. *Science*, *303*(5662), 1342–1345. https://doi.org/10.1126/science.1089424

Levy, R., & Hsu, C. (2015). MODIS atmosphere L2 aerosol product [Dataset]. *Goddard Space Flight Center*. https://doi.org/10.5067/MODIS/MOD04_L2.061

Liu, G., Li, J., Ying, T., Su, H., Huang, X., & Yu, Y. (2023). Increasing fire weather potential over Northeast China linked to declining Bering Sea ice. *Geophysical Research Letters*, *50*(19), e2023GL105931. https://doi.org/10.1029/2023gl105931

Liu, Y., Goodrick, S., & Heilman, W. (2014). Wildland fire emissions, carbon, and climate: Wildfire–climate interactions. *Forest Ecology and Management*, *317*, 80–96. https://doi.org/10.1016/j.foreco.2013.02.020

Magaritz-Ronen, L., & Raveh-Rubin, S. (2021). Wildfire smoke highlights troposphere-to-stratosphere pathway. *Geophysical Research Letters*, *48*(23), e2021GL095848. https://doi.org/10.1029/2021gl095848

NASA/LARC/SD/ASDC. (2018). CALIPSO Lidar level 2 aerosol profile, V4-21 [Dataset]. *NASA ASDC*. https://doi.org/10.5067/CALIOP/CALIPSO/CAL_LID_L2_05kmAPro-Standard-V4-21

National Centers for Environmental Information. (2023). Integrated surface database [Dataset]. *NASA ASDC*. Retrieved from https://www.ncei.noaa.gov/data/global-hourly/access

Péré, J. C., Bessagnet, B., Mallet, M., Waquet, F., Chiapello, I., Minvielle, F., et al. (2014). Direct radiative effect of the Russian wildfires and its impact on air temperature and atmospheric dynamics during August 2010. *Atmospheric Chemistry and Physics*, *14*(4), 1999–2013. https://doi.org/10.5194/acp-14-1999-2014

Peterson, D. A., Campbell, J. R., Hyer, E. J., Fromm, M. D., Kablick, G. P., Cossuth, J. H., & DeLand, M. T. (2018). Wildfire-driven thunderstorms cause a volcano-like stratospheric injection of smoke. *npj Climate and Atmospheric Science*, *1*(1), 30. https://doi.org/10.1038/s41612-018-0039-3

Reid, C. E., Brauer, M., Johnston, F. H., Jerrett, M., Balmes, J. R., & Elliott, C. T. (2016). Critical review of health impacts of wildfire smoke exposure. *Environmental Health Perspectives*, *124*(9), 1334–1343. https://doi.org/10.1289/ehp.1409277

Shi, H., Jiang, Z., Zhao, B., Li, Z., Chen, Y., Gu, Y., et al. (2019). Modeling study of the air quality impact of record-breaking Southern California wildfires in December 2017. *Journal of Geophysical Research: Atmospheres*, *124*(12), 6554–6570. https://doi.org/10.1029/2019jd030472

Sokolik, I. N., Soja, A. J., DeMott, P. J., & Winker, D. (2019). Progress and challenges in quantifying wildfire smoke emissions, their properties, transport, and atmospheric impacts. *Journal of Geophysical Research: Atmospheres*, *124*(23), 13005–13025. https://doi.org/10.1029/2018jd029878

Stein, A. F., Draxler, R. R., Rolph, G. D., Stunder, B. J. B., Cohen, M. D., & Ngan, F. (2015). NOAA's HYSPLIT atmospheric transport and dispersion modeling system. *Bulletin of the American Meteorological Society*, *96*(12), 2059–2077. https://doi.org/10.1175/bams-d-14-00110.1

Tosca, M. G., Randerson, J. T., & Zender, C. S. (2013). Global impact of smoke aerosols from landscape fires on climate and the Hadley circulation. *Atmospheric Chemistry and Physics*, *13*(10), 5227–5241. https://doi.org/10.5194/acp-13-5227-2013

Urbanski, S. (2014). Wildland fire emissions, carbon, and climate: Emission factors. *Forest Ecology and Management*, *317*, 51–60. https://doi.org/10.1016/j.foreco.2013.05.045

U.S. Environmental Protection Agency. (2023). Air quality system data mart [Dataset]. *United States Environmental Protection Agency*. Retrieved from https://www.epa.gov/outdoor-air-quality-data

Wang, J., Su, H., Wei, C., Zheng, G., Wang, J., Su, T., et al. (2023). Black-carbon-induced regime transition of boundary layer development strongly amplifies severe haze. *One Earth*, *6*(6), 751–759. https://doi.org/10.1016/j.oneear.2023.05.010

Wang, Z., Huang, X., & Ding, A. (2018). Dome effect of black carbon and its key influencing factors: A one-dimensional modelling study. *Atmospheric Chemistry and Physics*, *18*(4), 2821–2834. https://doi.org/10.5194/acp-18-2821-2018

Wang, Z., Huang, X., & Ding, A. (2019). Optimization of vertical grid setting for air quality modelling in China considering the effect of aerosol-boundary layer interaction. *Atmospheric Environment*, *210*, 1–13. https://doi.org/10.1016/j.atmosenv.2019.04.042

Wang, Z., Huang, X., Wang, N., Xu, J., & Ding, A. (2020). Aerosol-radiation interactions of dust storm deteriorate particle and ozone pollution in East China. *Journal of Geophysical Research: Atmospheres*, *125*(24), e2020JD033601. https://doi.org/10.1029/2020jd033601

Wang, Z., Wang, Z., Zou, Z., Chen, X., Wu, H., Wang, W., et al. (2023). Severe global environmental issues caused by Canada's record-breaking wildfires in 2023. *Advances in Atmospheric Sciences*, *41*(4), 565–571. https://doi.org/10.1007/s00376-023-3241-0

Westerling, A. L., Hidalgo, H. G., Cayan, D. R., & Swetnam, T. W. (2006). Warming and earlier spring increase western U.S. forest wildfire activity. *Science*, *313*(5789), 940–943. https://doi.org/10.1126/science.1128834

Wiedinmyer, C., & Emmons, L. (2022). Fire Inventory from NCAR version 2 fire emission [Dataset]. *NCAR*. https://doi.org/10.5065/XNPA-AF09

Wiedinmyer, C., Kimura, Y., McDonald-Buller, E. C., Emmons, L. K., Buchholz, R. R., Tang, W., et al. (2023). The Fire Inventory from NCAR version 2.5: An updated global fire emissions model for climate and chemistry applications [Dataset]. *Geoscientific Model Development*, *16*(13), 3873–3891. https://doi.org/10.5194/gmd-16-3873-2023

Young, S. A., Vaughan, M. A., Kuehn, R. E., & Winker, D. M. (2013). The retrieval of profiles of particulate extinction from Cloud–Aerosol Lidar and Infrared Pathfinder Satellite Observations (CALIPSO) data: Uncertainty and error sensitivity analyses. *Journal of Atmospheric and Oceanic Technology*, *30*(3), 395–428. https://doi.org/10.1175/jtech-d-12-00046.1

Zeng, L., Tan, T., Zhao, G., Du, Z., Hu, S., Shang, D., & Hu, M. (2024). Overestimation of black carbon light absorption due to mixing state heterogeneity. *npj Climate and Atmospheric Science*, *7*(1), 2. https://doi.org/10.1038/s41612-023-00535-8

Zheng, B., Ciais, P., Chevallier, F., Yang, H., Canadell, J. G., Chen, Y., et al. (2023). Record-high CO_2 emissions from boreal fires in 2021. *Science*, *379*(6635), 912–917. https://doi.org/10.1126/science.ade0805

Zheng, G., Sedlacek, A. J., Aiken, A. C., Feng, Y., Watson, T. B., Raveh-Rubin, S., et al. (2020). Long-range transported North American wildfire aerosols observed in marine boundary layer of eastern North Atlantic. *Environment International*, *139*, 105680. https://doi.org/10.1016/j.envint.2020.105680